**Atmospheric
Chemistry
and Physics**

On using radon-222 and CO_2 to calculate regional-scale CO_2 fluxes

A. I. Hirsch

Cooperative Institute for Research in Environmental Sciences, University of Colorado, Boulder, Colorado, USA

NOAA/ESRL Global Monitoring Division, Boulder, Colorado, USA

Abstract. Because of its ubiquitous release on land and well-characterized atmospheric loss, radon-222 has been very useful for deducing fluxes of greenhouse gases such as CO_2, CH_4, and N_2O. It is shown here that the radon-tracer method, used in previous studies to calculate regional-scale greenhouse gas fluxes, returns a weighted-average flux (the flux field F weighted by the sensitivity of the measurements to that flux field, f) rather than an evenly-weighted spatial average flux. A synthetic data study using a Lagrangian particle dispersion model and modeled CO_2 fluxes suggests that the discrepancy between the sensitivity-weighted average flux and evenly-weighted spatial average flux can be significant in the case of CO_2, due to covariance between F and f for biospheric CO_2 fluxes during the growing season and also for anthropogenic CO_2 fluxes in general. A technique is presented to correct the radon-tracer derived fluxes to yield an estimate of evenly-weighted spatial average CO_2 fluxes. A new method is also introduced for correcting the CO_2 flux estimates for the effects of radon-222 radioactive decay in the radon-tracer method.

1 Introduction

Radon-222 has proven to be useful for atmospheric research in several ways (see Zahorowski et al., 2004 for a review), mainly for evaluating regional and global chemical transport models (CTMs) (see references in Zahorowski et al., 2004; Gupta et al., 2004; Krol et al., 2005), estimating regional fluxes of chemically and radiatively important gases such as CO_2 (Levin, 1987; Gaudry et al., 1990; Schmidt et al., 1996, 2003; Biraud et al., 2000; Levin et al., 2003), CH_4 (Schmidt et al., 1996; Levin et al., 1999; Biraud et al., 2000), and N_2O (Wilson et al., 1997; Schmidt et al., 2001), and estimating

the exchange of CO_2 between forest canopies and the atmosphere (Trumbore et al., 1990; Ussler et al., 1994; Martens et al., 2004). This study focuses on the use of radon-222 to infer regional-scale fluxes of CO_2, the gas responsible for the majority of the direct greenhouse forcing increase over pre-industrial times. The principle behind this application is that radon-222 and CO_2 are both exchanged between the biosphere and the atmosphere near the Earth's surface and undergo the same atmospheric mixing processes. The radon-222 flux is thought to be fairly well known and uniform so that it can be used to "calibrate" the CO_2 flux. In this approach, the radon-222 flux is multiplied either by the ratio of the discrepancies of CO_2 and radon-222 from remote background concentrations (Levin, 1987; Levin et al., 2003; Schmidt et al., 2003) or by the linear slope of a CO_2/radon-222 plot (Gaudry et al., 1990; Schmidt et al., 1996; Biraud et al., 2000; Schmidt et al., 2001). Using the linear slope only appears to work outside of the growing season, when CO_2 and radon-222 fluxes have similar spatio-temporal variability (both are fairly uniform and directed from the biosphere to the atmosphere). This paper is an extension of both varieties of the radon-tracer method. It is shown that during the growing season, regional-scale CO_2 fluxes can be calculated using a single pair of radon-222 and CO_2 measurements, removing the need for a large collection of well-correlated measurements. It will also be shown that the radon-tracer method returns a weighted-average CO_2 flux (weighted by f, the sensitivity of measurements to the flux field) rather than an evenly-weighted spatial average; due to covariance between the CO_2 flux and f, the two can be quite different. This conclusion appears to hold true for both biospheric and anthropogenic CO_2 fluxes. A new method is presented to diagnose this covariance term and also to account for the impact of radioactive decay of radon-222 on the CO_2 flux estimates.

Correspondence to: A. I. Hirsch
(adam.hirsch@noaa.gov)

2 Methods

2.1 Gridded flux data sets used in this study

A monthly-average diurnal cycle (six hour averages) of NEE (Net Ecosystem Exchange of CO_2) for the months of July and September 2000 was calculated from hourly NEE predicted by the SiB2 model (Sellers et al., 1996a,b; Denning et al., 1996; Schaefer et al., 2002) at $1° \times 1°$ spatial resolution for North America. This diurnal cycle was repeated each day in a "cyclostationary" setup as a bottom boundary condition to generate CO_2 mixing ratios, as described below. A constant, spatially uniform 1 atom cm^{-2} s^{-1} (1.66×10^{-14} μmol m^{-2} s^{-1}) flux was assumed for radon-222. To generate fossil fuel CO_2 mixing ratios, the EDGAR 32FT2000 gridded $1° \times 1°$ data set of fossil CO_2 flux (http://www.mnp.nl/edgar/model/v32ft2000edga) was used as a bottom boundary condition. In this paper all mole fraction units are presented as ppm (10^{-6} mol mol^{-1}) and all flux units as μmol m^{-2} s^{-1}.

2.2 "Concentration footprint" and synthetic data generation

The 6-hourly synthetic CO_2 and radon-222 data were generated using the "concentration footprint" (Gloor et al., 2001) for each measurement. The concentration footprint, also called the "upstream surface influence function" (Lin et al., 2003) or "field of view" of a measurement station (Siebert and Frank, 2004), quantifies the sensitivity of each measurement to the near-field surface fluxes upwind of the measurement site. For simplicity, they will be called "footprints" in the remainder of the paper. The footprints are calculated with the Stochastic Time-Inverted Lagrangian Transport (STILT) model (Lin et al., 2003) using:

$$f\left(\boldsymbol{x}_r, t_r | x_i, y_i, t_m\right) = \frac{m_{\text{air}}}{h\overline{\rho}\left(x_i, y_i, t_m\right)} \frac{1}{N_{\text{tot}}} \sum_{p=1}^{N_{\text{tot}}} \Delta t_{p,i,j,k} \quad (1)$$

The left hand side of (1) is the concentration response (ppm) at the receptor (i.e. the measurement site, located at $\mathbf{x}_r$ and at time t_r) to a flux (μmol m^{-2}s^{-1}) from an area of the Earth's surface centered at (x_i, y_i) at time t_m. The first term on the right hand side represents the concentration response due to dilution of a surface flux into the lower part of the planetary boundary layer (assumed to be well mixed in one model time step) of height h. m_{air} is the molar mass of air and $\overline{\rho}$ is the average density of air below h. Please see Lin et al. (2003) for details of the STILT model, including how h is determined. The rest of the right hand side represents the time- and space-integrated particle density of the particles transported back in time that lie in the lower part of the boundary layer, normalized by the total number of particles released. Thus we would expect greater sensitivity to surface fluxes when the boundary layer is relatively shallow and horizontal wind speeds are slow. For this study, 5-day

back-trajectories of 300 particles each were run back every six hours from 25 m above ground level at the location of the ARM-CART (Atmospheric Radiation Measurement — Cloud And Radiation Testbed) SGP (Southern Great Plains) 60 meter tower (37.5 N, 97.5 W) for 25 days in the months of July and September 2004. Winds from 2004 were chosen because of the high resolution available; while these winds are not totally consistent with the meteorology driving SiB2, the same winds are used both to generate the synthetic data and to deduce fluxes from that synthetic data. The ARM-CART site was chosen because continuous PBL (Planetary Boundary Layer) radon-222 measurements commenced there in October, 2006. High precision CO_2 measurements at 2 meters, 4 m, 25 m, and 60 m are ongoing at the site as are eddy covariance measurements of NEE at 4, 25, and 60 m (http://www-esd.lbl.gov/ARMCarbon) as well as a multitude of other experiments designed to understand boundary layer dynamics (http://arm.gov/sites/sgp.stm). The 25 m height was chosen to simulate measurements from a height similar to that used in short-tower eddy covariance studies. Results for July using 500 m above ground level to simulate tall tower measurements are also presented for comparison. STILT was driven by 40 km EDAS winds from NCEP on the North American continent, and 180 km NCEP FNL winds further away. No cloud convection was included in this "perfect transport" experiment (again, the same wind fields are used to generate the synthetic data and to deduce CO_2 fluxes). Clearly, if one wants to analyze real data that are influenced by deep convection, a more realistic treatment of cloud convection would be necessary. Here we are simply testing the hypothesis that covariance between fluxes and measurement footprints can influence the fluxes inferred by the radon-tracer method in the absence of deep convection. The footprints were calculated on a $1° \times 1°$ grid using (1) for 0–6, 6–12, 12–18, etc. hours back in time before the corresponding measurement time. The average footprint for the July 500 m measurements is shown as an example (Fig. 1).

By calculating the footprints for the individual 6-h intervals leading up to a given measurement, it is straightforward to apply a radioactive decay correction to simulate radon-222 decay during transit to the measurement site (using an exponential decay term with a 5.5 day e-folding time). The synthetic measurements for both radon-222 and CO_2 were generated using a simple matrix multiplication:

$$\boldsymbol{z} = \mathbf{H}\boldsymbol{s} \quad (2)$$

The vector $\mathbf{z}$ contains the synthetic measurements (25 days $\times$ 4 day^{-1} = 100 elements), the vector $\boldsymbol{s}$ contains the surface fluxes (4 day^{-1} $\times$ ~2000 grid cells in the domain ~8000 elements), and the matrix $\mathbf{H}$ (dimensioned 100$\times$8000) is the sensitivity of the measurements to the fluxes, calculated using (1). The vector $\boldsymbol{z}$ represents the modification of "background" CO_2 or radon-222 mole fractions by terrestrial fluxes near the measurement site. No error was added to the
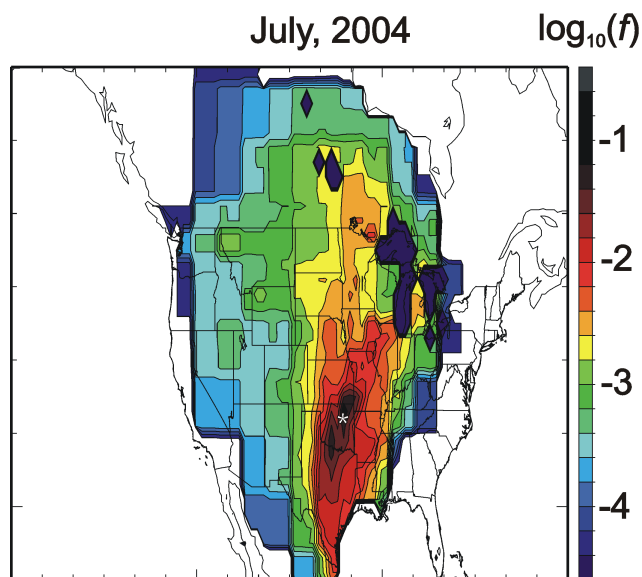
Fig. 1. Logarithm of the average footprint (ppm $(\mu\text{mol}\,\text{m}^{-2}\,\text{s}^{-1})^{-1}$) for July measurements at 500 m. Approximate location of ARM-CART SGP denoted by star. The Great Lakes and other water bodies were given a value of zero.

synthetic measurements; however, the uncertainty of the retrieved CO$_2$ fluxes is diagnosed below.

2.3 Correcting for the effect of radon-222 decay

The 5-day flux footprint values far from the tower will be smaller for radon-222 than for an inert tracer with the same flux since the radon-222 signal in the boundary layer is diminished by radioactive decay. In order to use radon-222 to calculate CO$_2$ fluxes, the radon-222 data must be corrected for the effects of radioactive decay; otherwise, CO$_2$ fluxes calculated by the radon-tracer method will be overestimated (i.e., radioactive decay will be interpreted as extra dilution by free tropospheric air). A scatter plot of two different radon-222 synthetic data sets (one generated by the CTM including radioactive decay, one without radioactive decay to simulate an inert tracer) shows a compact linear relationship (Table 1) during July at 25 and 500 m, and during September at 25 m. Using the regression coefficients (Table 1), radon-222 can be transformed into a "conserved" tracer for use in the radon-tracer technique. This approach is different from that used in Schmidt et al. (2001) which applied a correction to the radon-222 data based on an assumed transit time of boundary layer across a continent. These results suggest that neglecting the impact of radioactive decay on radon-222 concentrations during transit of air to the measurement site can lead to overestimation of the CO2 flux by ≥10% if they do not account for radioactive decay of radon-222. The overestimate during September would be ∼20%, and the July overestimate using 500 m measurements would be almost 50%. The correction

Table 1. Linear fit coefficients of a scatterplot of radon-222 simulated without radioactive decay versus radon-222 simulated with radioactive decay.

Time	Slope, ppm ppm^{-1}	Intercept, ppm$\times 10^{15}$	R^2
July 25 m	1.12±0.02	6.2±1.3	0.97
July 500 m	1.47±0.03	−3.7±1.2	0.96
September 25 m	1.18±0.02	4.5±1.6	0.97

at 25 m agrees with earlier efforts to account for the influence of radon-222 decay (Schmidt et al., 2001, 2003), but the 500 meter correction is large in comparison. Further work is required to diagnose the influence of cloud convection on these results.

2.4 Mathematical background

Two different quantities are defined here for use below: 1) the footprint-weighted CO$_2$ flux, which is the CO$_2$ flux field F weighted by the footprint sensitivities f:

$$F_{\text{co}_2} = \frac{\sum_{i=1}^{n} F_{i,\text{co}_2}\, f_i}{\sum_{i=1}^{n} f_i} \tag{3}$$

where the flux F in grid cell i is weighted by f in that grid cell, and 2) the evenly-weighted footprint-average flux, which is an average over the geographical area encompassed by the footprint:

$$\overline{F_{\text{co}_2}} = \frac{1}{n} \sum_{i=1}^{n} F_{i,\text{co}_2} \tag{4}$$

The CO$_2$ flux is calculated in the radon-tracer technique as:

$$F_{\text{co}_2,Rn} = \overline{F_{Rn}} \frac{\Delta\,[\text{CO}_2]}{\Delta\,[^{222}Rn^*]} \tag{5}$$

$F_{\text{co}_2,Rn}$ is the flux of CO$_2$ inferred from radon-222; $\overline{F_{Rn}}$ is the average flux of radon-222 in the footprint; the Δ terms in brackets represent the mixing ratio enhancements over (or depletions below) background levels of CO$_2$ and radon-222 respectively, where ^{222}Rn* is radon-222 adjusted to remove the effect of radioactive decay. Generally, long-term averages are used; we show here that a meaningful regional-scale CO$_2$ flux estimate can be derived from a single pair of $\Delta[\text{CO}_2]$ and $\Delta[^{222}$Rn*]. The ratio of the Δ terms can also represent the slope of a CO$_2$/radon-222 plot, as mentioned above. In this study, the background mixing ratios are assumed to be perfectly known (a source of uncertainty that needs to be addressed in future work). Because the radon-222 flux is assumed here to be uniform in space and time

(a standard assumption that also requires further study), $\Delta [^{222}Rn*]$ can be expressed as:

$$\Delta \left[^{222}Rn* \right] = \overline{F_{Rn}} \sum_{i=1}^{n} f_i \quad (6)$$

The summation in (6) applies to the values of f in all n grid cells in the footprint of a given measurement. We see from (6) that dividing the $\Delta[^{222}Rn*]$ by the radon-222 flux provides information about boundary layer dynamics as they are reflected in f. The situation is different for CO_2 because both F and f vary within a footprint:

$$\Delta [CO_2] = \sum_{i=1}^{n} \left[F_{i,co_2} f_i \right] = \sum_{i=1}^{n} \left[\left(\overline{F_{co_2}} + F'_{i,co_2} \right) \left(\overline{f} + f'_i \right) \right] (7)$$

The first thing to notice is that if (6) and (7) are substituted into (5), we find:

$$F_{co_2, Rn} = \frac{\sum_{i=1}^{n} F_{i,co_2} f_i}{\sum_{i=1}^{n} f_i} \quad (8)$$

This equation is identical to (3); therefore, we can conclude that the radon-tracer equation (5) yields a footprint-weighted flux, rather than an evenly-weighted spatial average flux.

In (7), F'_i and f'_i represent the deviations of the CO_2 flux and the footprint sensitivity values from their (evenly-weighted) mean values in the footprint, $\overline{F}$ and $\overline{f}$ respectively. By definition, $\sum_{i=1}^{n} \left(F'_{i,co_2} \right) = 0$, $\sum_{i=1}^{n} \left(f'_{i,co_2} \right) = 0$, and $\sum_{i=1}^{n} \overline{f} = \sum_{i=1}^{n} f_i$ so that (7) is equivalent to:

$$\Delta [CO_2] = \overline{F_{co_2}} \sum_{i=1}^{n} f_i + \sum_{i=1}^{n} \left(F'_{i,co_2} f'_i \right) \quad (9)$$

Dividing by $\sum_{i=1}^{n} f_i$ and combining (5), (6), and (9), we derive:

$$F_{co_2, Rn} = \overline{F_{co_2}} + \frac{\sum_{i=1}^{n} \left(F'_{i,co_2} f'_i \right)}{\sum_{i=1}^{n} f_i} \quad (10)$$

From (10) we see that using radon-222 and CO_2 measurements in the radon-tracer method will only yield the evenly weighted footprint-average CO_2 flux (the first term on the right hand side of Eq. 10) if the covariance between F and f (the second term on the right hand side of Eq. 10) is zero. While it is recognized that the second term on the right hand side is normalized by $\sum_{i=1}^{n} f_i$ rather than by n and thus not technically a covariance, the numerator is the same and therefore this term will be called the "covariance term" for convenience. Equations (5) and (10) present a way to correct

the radon-tracer derived flux for the covariance term to yield the evenly-weighted footprint-average CO_2 flux (equivalent to Eq. 4):

$$\overline{F_{co_2}} = \overline{F_{Rn}} \frac{\Delta [CO_2]}{\Delta \left[^{222}Rn* \right]} - \frac{\sum_{i=1}^{n} \left(F'_{i,co_2} f'_i \right)}{\sum_{i=1}^{n} f_i} \quad (11)$$

Using (11) requires an accurate estimate of the spatio-temporal variability of F and f around their footprint-average values, provided by transport model and biogeo-chemical model calculations. As will be shown below, the impact of covariance between F and f can be quite large compared to the mean NEE and fossil fuel CO_2 flux, even in the monthly mean. The second term on the right hand side of (11) can also be used conservatively to screen out times where the covariance term is large, so that the CO_2 flux estimated using (5) would yield an accurate result for the footprint-average value.

3 Results

3.1 Deducing NEE using radon-222 and CO_2

First, the synthetic radon-222 (Fig. 2a) and CO_2 time series generated with SiB2 (Fig. 2b) NEE are shown. Radon-222 is shown in the somewhat unconventional units of ppm ($\times 10^{13}$), for comparison with CO_2. Radon-222 sampled at 25 m is similar in July and September with occasionally higher nocturnal accumulation in September. In both July and September, the diurnal cycle at 25 m is pronounced. The midday mixing ratios of radon-222 at 25 m and 500 m are similar in July, indicating well-mixed conditions; the diurnal variability at 500 m is much smaller than near the surface. The synthetic CO_2 time series show more differences between July and September than for radon-222. In September, the diurnal variability is still large; however, the average mixing ratio is much higher than the background than in July because of weaker photosynthetic uptake during autumn. Plots of synthetic CO_2 versus synthetic radon-222 (Fig. 3) show a strong correlation during September at 25 m ($R^2 = 0.91$, intercept = -2.8 ± 0.5 ppm, slope = $2.2 \times 10^{14} \pm 6.8 \times 10^{12}$ ppm CO_2 (ppm radon-222)$^{-1}$, equivalent to ~ 4 ppm CO_2 per Bq m^{-3} of radon-222 at standard temperature and pressure), poorer correlation in July at 25 m ($R^2 = 0.52$), and especially poor correlation in July at 500 m ($R^2 \sim 0$).

Next, the evenly-weighted footprint-average CO_2 fluxes predicted by the SiB2 model are shown (Fig. 4a) for each measurement. These values represent the "truth" that we are trying to deduce with the radon-222 and CO_2 time series using the radon-tracer method. In September, the mean flux is always positive and does not show much day-to-day variability. In July, the mean NEE is generally negative (uptake
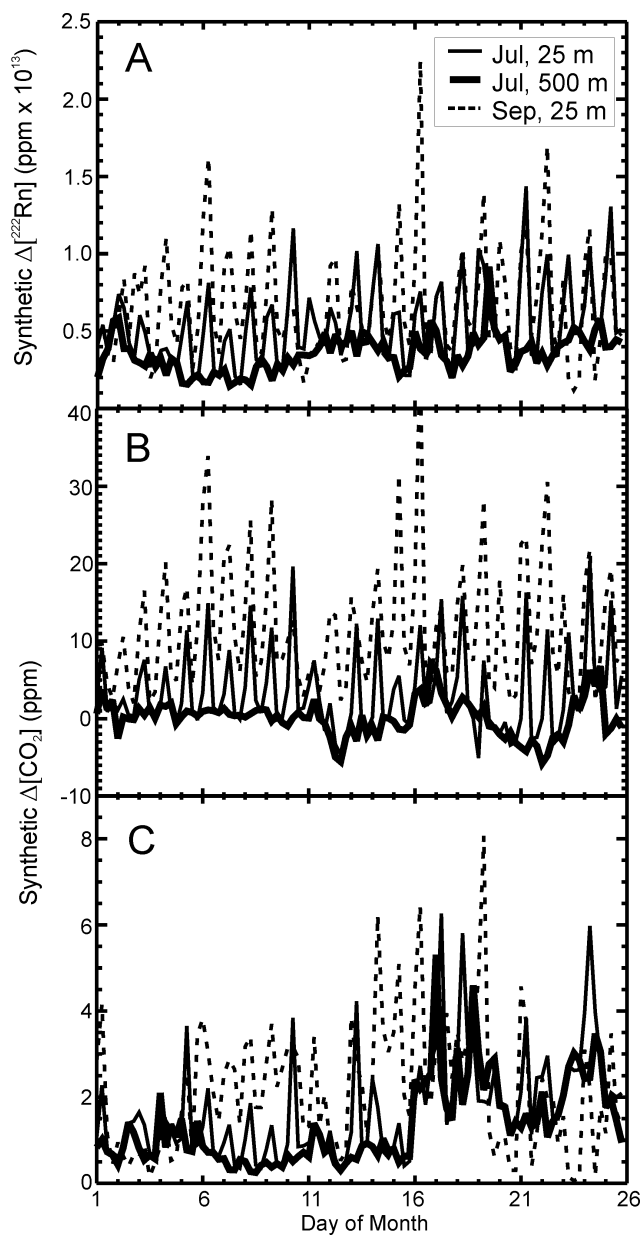
Fig. 2. (A) Time series of synthetic radon-222 sampled in the model at the location of the ARM-CART SGP 60 m tower during July at 25 m (thin solid), 500 m (thick solid) and during September at 25 m (dashed). **(B)** Time series of synthetic CO_2 generated with SiB2 fluxes. **(C)** Time series of synthetic CO_2 generated with EDGAR flux inventory.

of atmospheric CO_2) and shows considerable synoptic variability. During this period, different wind directions sample areas of the continent having different NEE, due to differences in ecosystem type, meteorology, or both. The results for 25 m and 500 m in July are similar except for some time periods where they differ by more than $1 \, \mu$mol m^{-2} s^{-1}. The difference in the footprint-mean NEE for 25 meter and 500 m measurements is greatest at night; this should be expected
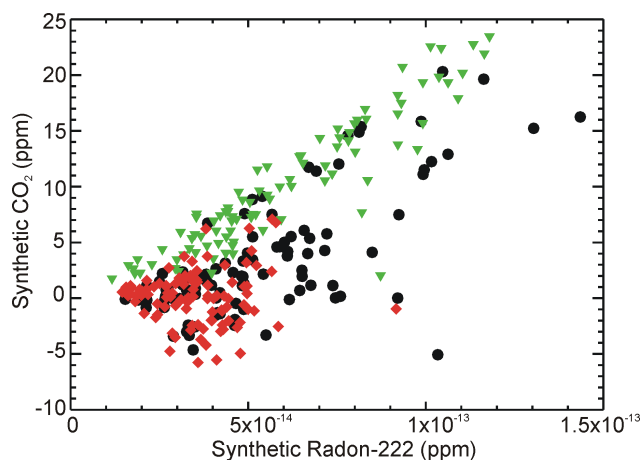

Fig. 3. Plots of CO_2 versus radon-222 during July at 25 m (black circles), July at 500 m (red diamonds), and September at 25 m (green triangles).

given that the 500 m sampling height is generally above the nocturnal boundary layer, and may receive air from a different direction. These fluxes represent the average NEE in the footprint of each measurement during the five days leading up to the measurement.

Once the radon-222 is "corrected" for radioactive decay, the two terms on the right hand side of (11) can be calculated (called here "first term on the RHS of (11)" and "the covariance term" respectively, where "RHS" stands for "Right Hand Side"). The first term on the RHS of (11), which is the same as (5), looks quite different from the evenly-weighted footprint-average NEE (Fig. 4b compared with 4a). This conclusion holds true even in September, when CO_2 and radon-222 appear to be well correlated (see Fig. 3). In July at 25 m, the first term on the RHS of (11) is generally higher than the evenly-weighted average NEE and shows much greater diurnal variability. Even during midday, when the PBL is well mixed, there are large discrepancies. The same holds true in September at 25 meters – a surprising result since the activity of the biosphere might be expected to be less vigorous in autumn, as reflected in the strong correlation between CO_2 and radon-222 (Fig. 3). Using a sampling height of 500 meters, the first term on the RHS of (11) agrees much better with the footprint-average NEE. However there are still many periods when differences exceed $1 \, \mu$mol m^{-2} s^{-1}.

When calculated using the July 25 meter synthetic data, the covariance term (Fig. 4c) shows a large diurnal cycle, with high values at night. It makes sense that the nighttime values of the covariance term are very large, because positive NEE (transfer of CO_2 to the atmosphere) near the tower is paired with very stable conditions. The average of the midday covariance term values is close to zero in July (although the value exceeds $1 \, \mu$mol m^{-2} s^{-1} on some days) but the covariance term is always large and positive in September.
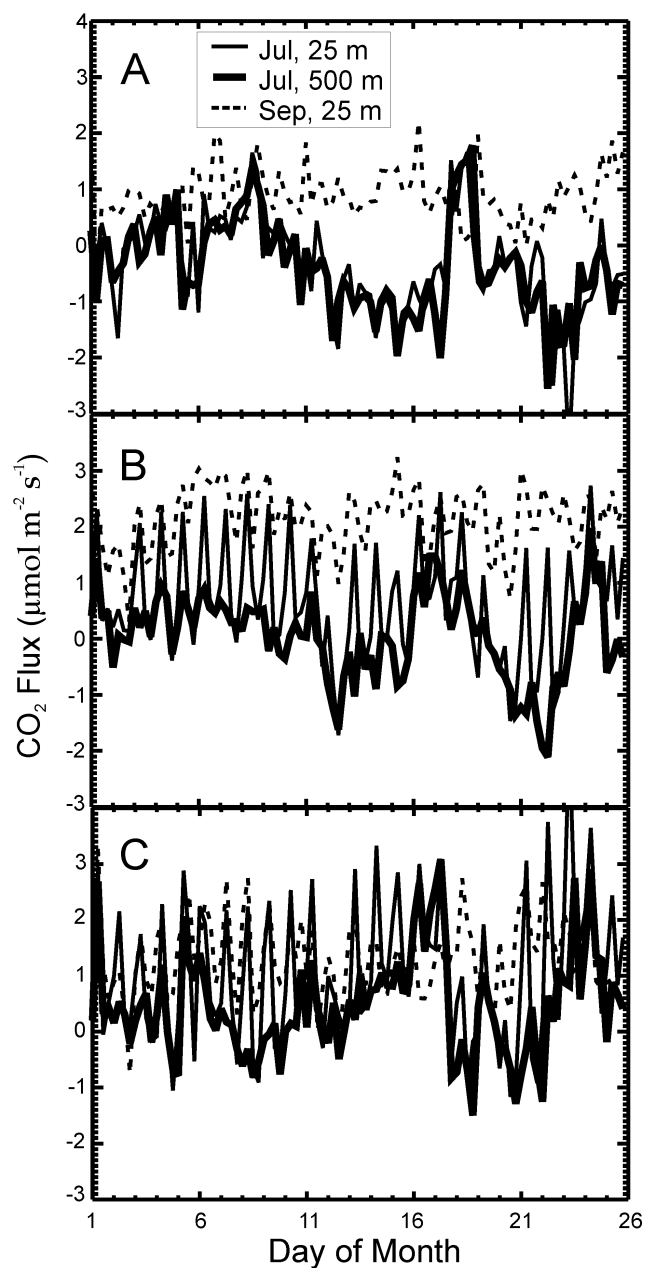
Fig. 4. (A) The evenly-weighted footprint-average NEE predicted by SiB2 for the measurements shown in Fig. 2. Line types correspond to those used in Fig. 2; **(B)** The footprint-mean NEE calculated using the first term on the right-hand side of (11) or (5); **(C)** The value of the covariance term.

Table 2. Comparison between evenly-weighted NEE and covariance term.

Time	Average NEE μmol m^{-2} s^{-1}	Average Covariance Term μmol m^{-2} s^{-1}
July 25 m all hours	−0.4	1.0
July 25 m 12:00–18:00 LT	−0.1	0.1
July 500 m all hours	−0.4	0.5
July 500 m 12:00–18:00 LT	−0.2	0.1
September 25 m all hours	0.9	1.3
September 25 m 12:00–18:00 LT	1.0	0.9

the covariance term. The main point to take away is that the covariance term is generally of the same order of magnitude or larger than the first term on the RHS of (11). Thus a very large correction must be made to the result of (5) to yield the footprint-average NEE.

3.2 Deducing fossil fuel CO_2 emissions using radon-222 and $^{14}CO_2$

Since $^{14}CO_2$ measurements are becoming more precise and affordable, it makes sense to explore whether the approach presented here can be used to deduce the regional-scale flux of fossil fuel CO_2 using radon-222 (as done by Levin et al., 2003). Fossil fuel CO_2 contains no radiocarbon, so that the contribution of fossil fuel CO_2 to the total mixing ratio can be easily calculated from the difference between the $\Delta^{14}CO_2$ of a sample and the $\Delta^{14}CO_2$ of background air (Levin et al., 2003; Turnbull et al., 2006). Results are presented in the same order as for NEE. The mixing ratio enhancements from fossil fuel burning are smaller than the CO_2 variability introduced by NEE (Fig. 2c, compare with Fig. 2b). Interestingly, the footprint-average fossil fuel flux (Fig. 5a) is comparable to the footprint-mean NEE (see Fig. 4a). One can conclude that the fossil fuel CO_2 emissions are located relatively farther away from the tower than NEE, so that while the fluxes are comparable, the measurements are more diluted during transit to the measurement site. The first question to answer is whether the covariance term is significant in the case of fossil fuel CO_2. If there is no significant covariance term, we could just use (5) to calculate the fossil fuel CO_2 flux. However, in all three cases the covariance term (Fig. 5c) occasionally exceeds 0.5 μmol m^{-2} s^{-1}, compared to a flux that only reaches about 1.0 μmol m^{-2} s^{-1} at most (Fig. 5a). The monthly mean value of the covariance

Using 500 meter July data, the covariance term is smaller, shows less variability, and the monthly average is closer to zero for midday samples. However, the monthly mean value of the covariance term is always the same order of magnitude as the monthly mean flux, regardless of time of day (Table 2). Surprisingly, the midday mean value of the covariance term at 25 m is larger in September than in July. The reason is that in July, the mid-day points often include negative values of

term ranges from about $0.06 \, \mu\text{mol m}^{-2}\,\text{s}^{-1}$ (July, 25 m) to $0.1 \, \mu\text{mol m}^{-2}\,\text{s}^{-1}$ (July, 500 m) whereas the mean flux is only about $0.36 \, \mu\text{mol m}^{-2}\,\text{s}^{-1}$ during this period in all three cases. It appears that (as modeled here) covariance between the flux of fossil fuel CO_2 and f is significant. This conclusion is very interesting considering that we have included no diurnal variability in the fossil fuel flux. Just the fact that the anthropogenic emissions have a non-uniform spatial pattern raises the possibility that the footprint-average flux can differ from the footprint-weighted flux. During certain conditions, areas of relatively high (or low) emissions coincide with relatively high (or low) sensitivity of the measurements to those emissions. Only when averaged over very long time periods (>1 month) is this effect expected to approach zero, based on this analysis.

4 Discussion

4.1 Uncertainty analysis

Given uncertainties of the radon-222 flux, $\Delta^{14}CO_2$ measurements, and the covariance term, is there any hope of extracting a meaningful CO_2 flux using (11)? This issue is explored for NEE assuming the following: 25% relative precision on the radon-222 flux (Levin et al., 2003), 0.1 ppm precision on the CO_2 measurements, 3% relative precision on the hourly average radon-222 mixing ratio (Whittlestone and Zahorowski, 1998; Zahorowski et al., 2004), a 10% error in correcting the CO_2 flux for the influence of radon-222 radioactive decay caused by uncertainty in the regression coefficients, and assumed relative errors of 20% on F (both NEE and fossil fuel CO_2 flux) and f which are assumed to be uncorrelated. When applying the approach to fossil fuel CO_2, a different precision must be used for the fossil CO_2, which corresponds to the uncertainty of the radiocarbon measurement. One ppm of fossil fuel corresponds to: $(1/380)*(55+1000) = 2.8$‰, where 380 (ppm) is the current CO_2 mixing ratio (at Mauna Loa), 55 (‰) is the current $\Delta^{14}CO_2$ and -1000 (‰) is the $\Delta^{14}C$ of fossil fuel CO_2, which is subtracted from the present atmospheric radiocarbon activity. While the analytical uncertainty of the radiocarbon measurement is ~2‰, the detection limit of fossil fuel CO_2 using radiocarbon is $2.8/2.8 = 1$ ppm (i.e. $(2\times\sqrt{2})/2.8$ rather than $2/2.8$, since two measurements are needed to determine the difference between the sample value and a background value (J. B. Miller, NOAA/ESRL GMD, personal communication). The uncertainty of the first term on the RHS of (11) was calculated by simple error propagation. The uncertainty of the covariance term was calculated by taking the standard deviation of 100 realizations, adding normally distributed random errors to F and f. Using synthetic data from 25 m in July, the relative error on the first term on the RHS of (11) when solving for NEE has a median value of ~27%, but a mean value of 50%, due to select periods when
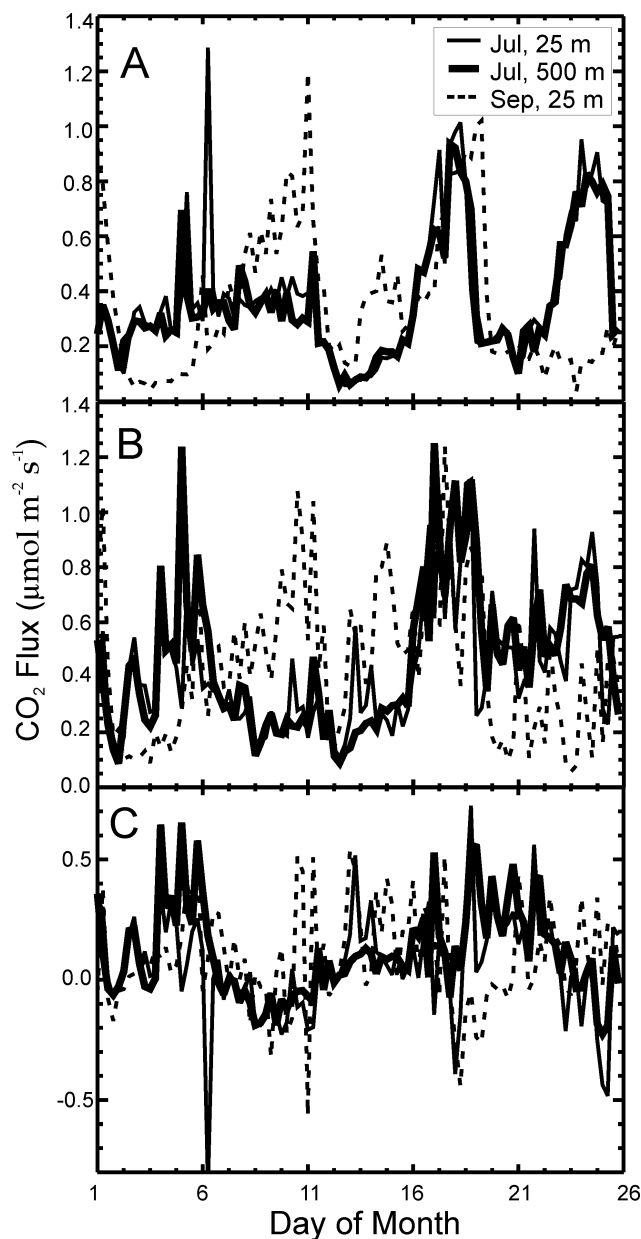
Fig. 5. (A) The footprint-average fossil fuel flux in the footprints of the synthetic data shown in Fig. 2c. **(B)** Same as 4b, except for fossil fuel fluxes; **(C)** Same as 4c, except for fossil fuel fluxes.

$\Delta[CO_2]$ is close to zero. Generally, the uncertainty of the first term on the RHS of (11) was larger for the fossil fuel case than for the NEE case because of the radiocarbon measurement uncertainty. Surprisingly, the uncertainty of the covariance term was comparable to the uncertainty of the first term on the RHS of (11), if not smaller. This uncertainty was relatively low because it is only when errors in F and f are correlated that the error accumulates rather than canceling out. It is unclear whether their errors are correlated or uncorrelated in reality. Since the biogeochemical models used
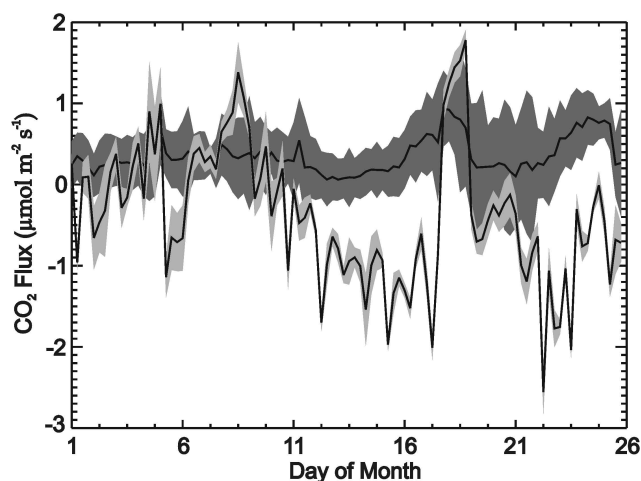
Fig. 6. Footprint-mean NEE (light error bounds) and fossil fuel CO_2 flux (dark error bounds) calculated using (11) for July measurements at 500 m, $\pm 1\sigma$.

to predict NEE are often driven by analyzed meteorological fields, it is possible that the errors are in fact correlated; however, diagnosing this issue is left to future work. It is expected that the errors in the fossil fuel flux and meteorological information will be uncorrelated, however. Overall, the uncertainty on the deduced fossil fuel flux is comparable to the uncertainty on the deduced NEE, using measurements at 25 m in July, because while the uncertainty of the first term on the RHS of (11) for fossil fuel is higher (due to the radiocarbon measurement uncertainty) the uncertainty on the covariance term is substantially lower. When the footprint-average fossil fuel CO_2 flux exceeds $\sim 0.3\,\mu\mathrm{mol\,m^{-2}\,s^{-1}}$ it can be distinguished from zero at the 1σ level. This flux threshold is higher for the 500 meter sampling level; the relative error on the fossil fuel CO_2 measurement is generally higher due to a more diluted signal. Interestingly, the periods with good signal to noise ratios of the derived flux do not always correspond to the measurements with the highest fossil CO_2 mixing ratio, since large fluxes can be substantially diluted before reaching the measurement location. Future studies will account for the uncertainty in the different components of f, such as the boundary layer height and horizontal wind components; this is the subject of on-going research (Lin and Gerbig, 2005).

The fossil fuel CO_2 flux and NEE deduced using the method presented here, along with the error bars derived above are shown for illustration for the fluxes derived from the July 500 m measurements (Fig. 6). There is enough variability in both fluxes so that despite fairly large uncertainties, the fluxes can be distinguished from zero and from each other, although the footprint-average fossil fuel flux needs to be rather large to be significantly different from zero even at 1σ. It is recognized that deducing fossil fuel CO_2 flux as presented here assumes measurement of fossil fuel CO_2 ev-

ery six hours, which is presently unfeasible. However, the approach could be applied to as many data points as could be afforded. Targeted sampling, perhaps triggered by CO mixing ratio increases caused by anthropogenic influence, is one possible approach. The approach presented here also presents a way to select samples for which the covariance term is likely to be very small and may be neglected.

4.2 Origins of covariance between F and f

First, the value of f will generally be much higher close to the sampling site, since the influence of fluxes farther away is erased by boundary layer flushing (see Fig. 1). Since the footprint sensitivities drop off exponentially with distance from the tower, CO_2 fluxes near the measurement site will be weighted much more strongly in $\Delta[CO_2]$ than fluxes farther away. Simply dividing $\Delta[CO_2]$ by the total sensitivity within the footprint will yield a footprint-weighted CO_2 flux which may be very different from the evenly-weighted footprint-average flux, as shown above. This phenomenon is known as "aggregation error" (Kaminski et al., 2001; Peylin et al., 2002). The "diurnal rectifier effect" (Denning et al., 1995, 1996; Yi et al., 2004; Chen et al., 2004, 2005) is a special case of aggregation error. Since NEE during the growing season can change sign between day and night, it is possible to have an average CO_2 flux within the footprint of zero. However, the factors (e.g. solar radiation) that control NEE also control PBL dynamics, such that NEE and the f covary. Therefore, it is often the case that $\Delta[CO_2]$ is not zero, despite the zero average NEE within the footprint, because some of the areas in the footprint are weighted more than others in the resulting CO_2 signal. This effect is well established, though its magnitude is uncertain. Preliminary modeling presented here (albeit using a single transport model and estimate of biospheric and anthropogenic fluxes) suggests that this covariance term appears to be of the same order of magnitude as the fluxes themselves during the growing season, and must be accounted for when inferring NEE or fossil fuel CO_2 flux using radon-222 (except for times when it is shown to be very small).

4.3 Comparison with other techniques to derive regional CO_2 fluxes

The approach presented here can be thought of as a very simple inverse model. It is more complex than simply using the radon-222 flux and the mixing ratios of radon-222 and CO_2 to get NEE yet simpler than Bayesian inverse modeling techniques. It has the disadvantage that it requires model predictions of the covariance between CO_2 fluxes and the surface influence function (although the rectifier effect must also be quantified for Bayesian inverse modeling studies). Yet it has the advantage that for a single radon-222 and CO_2 (or $^{14}CO_2$) measurement pair (or long-term averages), an evenly-weighted footprint-average value of NEE or fossil

fuel CO_2 emissions can be calculated. No error covariance matrices are required. The spatial extent of the footprint can be calculated using the transport model, so that it is easy to define the geographical area influencing a given set of measurements. The approach also has the advantage that no explicit prior flux values are required, just a prior knowledge of the covariance between the flux and transport. The method presented here, since it builds on the radon-tracer method, is also analogous to the boundary-layer budget technique of Bakwin et al. (2004), Helliker et al. (2004), and Betts et al. (2004). However, it has the added advantage of having the ability to identify the area for which the CO_2 flux is being calculated and more importantly, the covariance between F and f is accounted for. It is noted that it may be possible to neglect the covariance term if a tracer such as water vapor is used rather than radon-222, as suggested by the good agreement between the Helliker et al. (2004) boundary-layer budget calculations and eddy covariance NEE measurements. Since both CO_2 and water vapor are exchanged at plant stomata, their fluxes may have similar spatio-temporal variability (essentially, the covariance terms for the two gases cancel). Lastly, it is also recognized that the footprint-weighted flux returned by (5) could be a valuable quantity in its own right. However, the results of (5) should not be presented as an evenly-weighted footprint-average flux unless it is clear that the covariance term is small, either for a given measurement or on average over a long time period. There may even be times (as shown above) when CO_2 and radon-222 measurements are well correlated, yet the covariance term is quite large relative to NEE.

5 Conclusions and future work

This study is an extension of earlier work using radon-222 and CO_2 or $^{14}CO_2$ to calculate regional CO_2 fluxes. The technique presented here can be used to convert a footprint-weighted CO_2 flux from the radon-tracer technique to an evenly-weighted footprint-average flux by subtracting the influence of covariance between the surface fluxes and the sensitivity of CO_2 measurements to those fluxes. The method appears to be limited at this time by the uncertainties of the radon-222 flux and of the $\Delta^{14}CO_2$ measurements. The limit of detection for fossil fuel CO_2 emissions averaged over a footprint at the 1σ level is about $0.3\,\mu mol\,m^{-2}\,s^{-1}$ (although we have not considered uncertainty in the background CO_2 concentration here). It turns out that the limit of detection for NEE is about the same as for fossil fuel CO_2 emissions; lower uncertainty on the first term of the RHS of (11) is offset by higher uncertainty on the covariance term. To apply this technique (as in all techniques that use radon-222 to deduce CO_2 fluxes), it is necessary to "correct" the radon-222 measurements for radioactive decay. From modeling studies presented here, it appears that this correction is on the order of 10–20% near the surface, and higher aloft. It has also been shown that even during periods when CO_2 and radon-222 are highly correlated (September, 25 m), covariance between NEE and f can still lead to a discrepancy between the footprint-average and footprint-weighted NEE.

Several simplifying assumptions have been made in this study, such as ignoring variability in the background mixing ratios of radon-222 and CO_2, the spatio-temporal variability of the radon-222 flux (which could lead to covariance between the radon-222 flux and f), temporal variability of the fossil fuel flux, and the fossil fuel contribution to CO_2 when deducing NEE (if $^{14}CO_2$ measurements or some other reliable proxy for fossil fuel CO_2 are not available). The impact of including cloud convection in the CTM must also be diagnosed, or a way to exclude measurements influenced by deep convection must be developed. A study of how the spatial resolution of the footprints and NEE/fossil fuel emissions inventories affects the retrieved fluxes would also be helpful. All of these additional challenges are significant and need to be addressed in future work in order for this technique to be used with real data to deduce real fluxes. Multiple CTMs and multiple CO_2 flux datasets should be combined to explore how the modeled covariance between F and f might vary. It is likely that using this approach with night time measurements in the nocturnal boundary layer will require high-resolution mesoscale models, due to the difficulty of representing the dynamics of the nocturnal boundary layer in CTMs. Certainly, the covariance term will be smallest under well-mixed conditions at elevations high above the surface.

References

Bakwin, P. S., Davis, K. J., Yi, C., Wofsy, S. C., Munger, J. W., Haszpra, L., and Barcza, Z.: Regional carbon dioxide fluxes from mixing ratio data, Tellus, 56B, 301–311, 2004.

Betts, A. K., Helliker, B. R., and Berry, J. A.: Coupling between CO_2, water vapor, temperature and radon-222 and their fluxes in an idealized equilibrium boundary layer over land, J. Geophys. Res., D109, D18103, doi:10.1029/2003JD004420, 2004.

Biraud, S., Ciais, P., Ramonet, M., Simmonds, P., Kazan, V., Monfray, P., O'Doherty, S., Spain, T. G., and Jennings, S. G.: European greenhouse gas emissions estimated from continuous atmospheric measurements and radon 222 at Mace Head, Ireland, J. Geophys. Res., 105(D1), 1351–1366, 2000.

Chen, B., Chen, J. M., Liu, J., Chan, D., Higuchi, K., and Shashkov, A.: A Vertical Diffusion Scheme to estimate the atmospheric rectifier effect, J. Geophys. Res., 109, D04306, doi:10.1029/2003JD003925, 2004.

Chen, B., Chen, J. M., and Worthy, D. E. J.: Interannual variability in the atmospheric CO_2 rectification over a boreal forest region, J. Geophys. Res., 110, D16301, doi:10.1029/2004JD005546, 2005.

Denning, A. S., Fung, I. Y., and Randall, D.: Latitudinal gradient of atmospheric CO_2 due to seasonal exchange with land biota, Nature, 376, 240–243, 1995.

Denning, A. S., Collatz, G. J., Zhang, C., Randall, D. A., Berry, J. A., Sellers, P. J., Colello, G. D., and Dazlich, D. A.: Simulations of Terrestrial Carbon Metabolism and Atmospheric CO_2 in a General Circulation Model Part 1 Surface Carbon Fluxes, Tellus 48, 521–542, 1996.

Denning, A. S., Oren, R., McGuire, D., et al.: Science Implementation Strategy for the North American Carbon Program, Report of the NACP Implementation Strategy Group of the U.S. Carbon Cycle Interagency Working Group. Washington, DC: U.S. Carbon Cycle Science Program, 68 pp., 2005.

Gaudry, A., Polian, G., Ardouin, B., and Lambert, G.: Radon-calibrated emissions of CO_2 from South Africa, Tellus, 42B, 9–19, 1990.

Gloor, M., Bakwin, P., Hurst, D., Lock, L., Draxler, R., and Tans, P.: What is the concentration footprint of a tall tower?, J. Geophys. Res., 106(D16), 17 831–17 840, 2001.

Gupta, M. L., Douglass, A. R., Kawa, S. R., and Pawson, S.: Use of radon for evaluation of atmospheric transport models: sensitivity to emissions, Tellus, 56B, 404–412, 2004.

Helliker, B. R., Berry, J. A., Betts, A. K., Davis, K., Miller, J., Denning, A. S., Bakwin, P., Ehleringer, J., Butler, M. P., and Ricciuto, D.: Estimates of net CO_2 flux by application of equilibrium boundary layer concepts to CO_2 and water vapor measurements from a tall tower, J. Geophys. Res., D109, D20106, doi:10.1029/2004JD004532, 2004.

Kaminski, T., Rayner, P. J., Heimann, M., and Enting, I. G.: On aggregation errors in atmospheric transport inversions, J. Geophys. Res., 106(D5), 4703–4715, 2001.

Krol, M., Houweling, S., Bregman, B., van den Broek, M., Segers, A., van Velthoven, P., Peters, W., Dentener, F., and Bergamaschi, P.: The two-way nested global chemistry-transport zoom model TM5: algorithm and applications, Atmos. Chem. Phys., 5, 417–432, 2005,
http://www.atmos-chem-phys.net/5/417/2005/.

Levin, I.: Atmospheric CO_2 in continental Europe – an alternative approach to clean air CO_2 data, Tellus, 39B, 21–28, 1987.

Levin, I., Glatzel-Mattheier, H., Marik, T., Cuntz, M., and Schmidt, M.: Verification of German methane emission inventories and their recent changes based on atmospheric observations, J. Geophys. Res., 104(D3), 3447–3456, 1999.

Levin, I., Kromer, B., Schmidt, M., and Sartorius, H.: A novel approach for independent budgeting of fossil fuel CO_2 over Europe by $^{14}CO_2$ observations, Geophys. Res. Lett., 30(23), 2194, doi:10.1029/2003GL018477, 2003.

Lin, J. C. and Gerbig, C.: Accounting for the effect of transport errors on tracer inversions, Geophys. Res. Lett., 32, L01802, doi:10.1029/2004GL021127, 2005.

Lin, J. C., Gerbig, C., Wofsy, S. C., Andrews, A. E., Daube, B. C., Davis, K. J., and Grainger, C. A.: A near-field tool for simulating the upstream influence of atmospheric observations: the Stochastic Time-Inverted Lagrangian Transport (STILT) model, J. Geophys. Res., 108(D16), 4493, doi:10.1029/2002JD003161, 2003.

Martens, C. S., Shay, T., Mendlovitz, H. P., Matross, D. M., Saleska, S. R., Wofsy, S. C., Woodward, W. S., Menton, M. C., de Moura, J. M. S., Crill, P. M., de Moraes, O. L. L., and Lima, R. L.: Radon fluxes in tropical forest ecosystems of Brazilian Amazonia: night-time CO_2 net ecosystem exchange derived from radon and eddy covariance methods, Global Change Biol., 10, 618–629, doi: 10.1111/j.1529-8817.2003.00764.x, 2004.

Peylin, P., Baker, D., Sarmiento, J., Ciais, P., and Bousquet, P.: Influence of transport uncertainty on annual mean and seasonal inversions of atmospheric CO_2 data, J. Geophys. Res., 107(D19), 4385, doi:10.1029/2001JD000857, 2002.

Schaefer, K., Denning, A. S., Suits, N., Kaduk, J., Baker, I., Los, S., and Prihodko, L.: Effect of climate on interannual variability of terrestrial CO_2 fluxes, Global Biogeochem. Cycles, 16(4), 1101, doi:10.1029/2002GB001928, 2002.

Schmidt, M., Graul, R., Sartorius, H., and Levin, I.: Carbon dioxide and methane in continental Europe: a climatology and ^{222}Radon-based emissions estimates, Tellus, 48B, 457–473, 1996.

Schmidt, M., Glatzel-Mattheier, H., Sartorius, H., Worthy, D. E., and Levin, I.: Western European N_2O emissions: A top-down approach based on atmospheric observations, J. Geophys. Res., 106(D6), 5507–5516, 2001.

Schmidt, M., Graul, R., Sartorius, H., and Levin, I.: The Schauinsland CO_2 record: 30 years of continental observations and their implications for the variability of the European CO_2 budget, J. Geophys. Res., 108(D19), 4619, doi:10.1029/2002JD003085, 2003.

Sellers, P. J., Randall, D. A., Collatz, G. J., Berry, J. A., Field, C. B., Dazlich, D. A., Zhang, C., Collelo, G. D., and Bounoua, L.: A Revised Land Surface Parameterization of GCMs, Part I: Model Formulation, J. Climate, 9(3), 676–705, 1996a.

Sellers, P. J., Los, S. O., Tucker, C. J., Justice, C. O., Dazlich, D. A., Collatz, G. J., and Randall, D. A.: A Revised Land Surface Parameterization of GCMs, Part II: The Generation of Global Fields of Terrestrial Biophysical Parameters from Satellite Data, J. Climate, 9(3), 706–737, 1996b.

Siebert, P. and Frank, A.: Source-receptor matrix calculation with a Lagrangian particle dispersion model in backward mode, Atmos. Chem. Phys., 4, 51–63, 2004,
http://www.atmos-chem-phys.net/4/51/2004/.

Trumbore, S. E., Keller, M., Wofsy, S. C., and da Costa, J. M.: Measurements of Soil and Canopy Exchange Rates in the Amazon Rain Forest Using ^{222}Rn, J. Geophys. Res., 95(D10), 16 865–16 873, 1990.

Turnbull, J. C., Miller, J. B., Lehman, S. J., Sparks, R. J., and Tans, P. P.: Comparison of $^{14}CO_2$, CO, and SF_6 as tracers for recently added fossil fuel CO_2 in the atmosphere and implications for biological CO_2 exchange, Geophys. Res. Lett., 33, L01817, doi:10.1029/2005GL024213, 2006.

Ussler III, W., Chanton, J. P., Kelley, C. A., and Martens, C. S.: Radon 222 tracing of soil and forest canopy trace gas exchange in an open canopy boreal forest, J. Geophys. Res., 99, 1953–1963, 1994.

Whittlestone, S. and Zahorowski, W.: Baseline radon detectors for shipboard use: Development and deployment in the First Aerosol Characterization Experiment (ACE 1), J. Geophys. Res., 103(D13), 16 743–16 751, 1998.

Wilson, S. R., Dick, A. L., Fraser, P. J., and Whittlestone, S.: Nitrous oxide flux estimates for south-eastern Australia, Journal of Atmospheric Chemistry, 26, 169–188, 1997.

Yi, C., Davis, K. J., Bakwin, P. S., Denning, A. S., Zhang, N., Desai, A., Lin, J. C., and Gerbig, C.: Observed covariance between ecosystem carbon exchange and atmospheric boundary layer dynamics at a site in northern Wisconsin, J. Geophys. Res., 109, D08302, doi:10.1029/2003JD004164, 2004.

Zahorowski, W., Chambers, S. D., and Henderson-Sellers, A.: Ground based radon-222 observations and their application to atmospheric studies, J. Environ. Radioactivity, 76, 3–33, 2004.